

Electronic Supplementary Information (ESI)

Chemical substitution towards a rare-earth borate ultraviolet

NLO crystal exhibiting a strong SHG response

Xianghao Kong,^a Jing Chai,^a Huijian Zhao,^a Ning Ye,^a Zhanggui Hu,^a Yicheng Wu^a and Conggang Li^{*,a}

^aTianjin Key Laboratory of Functional Crystal Materials, Institute of Functional Crystal, Tianjin University of Technology, Tianjin 300384, China.

Corresponding Author* E-mail: cgli@email.tjut.edu.cn

1. Experimental Section

2. **Table S1** Crystallographic data and structural refinement for KLBO.
3. **Table S2** The final atomic coordinates ($\times 10^4$) and equivalent isotropic displacement parameters ($\text{\AA}^2 \times 10^3$) for KLBO, U_{eq} is defined as one-third of the trace of the orthogonalized U_{ij} tensor, and the bond valence sum (BVS) for each atom in asymmetric unit.
4. **Table S3** Bond lengths (\AA) and angles (deg.) for KLBO.
5. **Table S4** Direction and magnitude of the dipole moments in $\text{K}_{7.5}\text{Lu}_{2.5}\text{B}_{15}\text{O}_{30}$.
5. **Figure S1** Variable-temperature PXRD measurements of KLBO.
6. **Figure S2** Dihedral angle of the $[\text{B}_5\text{O}_{10}]$ groups in KLBO.

Experiment section

Synthesis. The high-temperature solid-phase reaction method was used, in which K_2CO_3 (Sinopharm, 99.9%), Lu_2O_3 (Sinopharm, 99.9%), and H_3BO_3 (Sinopharm, 99.9%) were used as starting materials, and K_2CO_3 , Lu_2O_3 , and H_3BO_3 were weighed according to established stoichiometric ratios, and were thoroughly ground with a mortar and pestle and put into a platinum crucible. The mixture was heated in a muffle furnace at $10^\circ\text{C min}^{-1}$ to 300°C for 10h and subsequently heated to 750°C and then sintered for 48 h before cooling to room temperature at 5°C min^{-1} . The purity of the resulting compounds was verified by powder X-ray diffraction (PXRD) analysis. KLBO single crystals were prepared using spontaneous crystallization technique. K_2CO_3 , Lu_2O_3 , Cs_2CO_3 , and H_3BO_3 were mixed in an established molar ratio, heated to 850°C , and held at this temperature for 10 h to ensure a homogeneous melt. Subsequently, KLBO crystals were formed by cooling the solution to 800°C at a rate of 1°C h^{-1} , then to 700°C at a rate of 3°C h^{-1} , and finally to room temperature by air cooling.

Powder XRD. PXRD analyses of the polycrystalline KLBO were carried out through a conventional Rigaku Smart Lab 9 kW diffractometer with monochromatized $\text{Cu K}\alpha$ radiation ($\lambda = 1.5418 \text{ \AA}$) recorded ranging from 10 to 70° at a step size of 0.01° with a step time of 2 s at room temperature.

Crystal preparation. Single crystals of KLBO were obtained by the spontaneous crystallization technique. Cs_2CO_3 was used as a flux to obtain the target single crystals. High quality and regular shape crystallized samples were selected for single crystal structure investigation. The crystallographic characteristics of KLBO crystals were recorded using a Bruker SMART APEX II 4K CCD diffractometer with $\text{Mo K}\alpha$ radiation at a wavelength of 0.71073 \AA and a temperature of $293(2) \text{ K}$ and processed using the SAINT program.¹⁻³ Detailed crystallographic information, including atomic coordinates, equivalence parameters, bond lengths, bond angles, and bond valences (BVS), is presented in Tables S1 and S2.

Optical property. The ultraviolet (UV) spectra of KLBO were obtained using a Hitachi UH4150 spectrophotometer with barium sulfate as the reference sample. The optical band gap of the compound was further estimated according to the Kubelka-Munk formula.⁴ In addition, the infrared spectrum of the compound was available at room temperature by using a STA6000-TL9000 FTIR spectrometer in the measured range of $400\text{--}4000 \text{ cm}^{-1}$. To prepare the test samples, the compound was completely mixed with KBr at a mass ratio of about 1 : 150, respectively.

Second-harmonic generation (SHG) characterization. In accordance with the Kurtz-Perry

methodology, the SHG of polycrystalline powders of KLBO was quantified at ambient temperature under an incident laser beam ($\lambda = 1064$ nm) emitted by a Q-switched Nd:YAG laser.⁵ Given that the SHG intensity of the powder is contingent upon the particle size range of the powder, pure polycrystalline samples of KLBO were screened and graded into the following distinct particle size ranges: 21-51, 51-74, 74-105, 105-125, 125-177, and 177-210 μm . Concurrently, a standard polycrystalline sample, KDP (KH_2PO_4), was also screened into the corresponding particle size ranges for relevant comparisons.

Computational details. The density functional theory (DFT) employed in the CASTEP package was utilized to implement *ab initio* calculations for KLBO. The Perdew-Burke-Ernzerhof (PBE) functional within the framework of the generalized gradient approximation (GGA) was applied.⁶⁻⁸ In the orbital electron analysis, the valence electrons of the KLBO compounds are considered, specifically those of K $3p^6 4s^1$, Lu $5d^1 6s^2$, B $2s^2 2p^1$, and O $2s^2 2p^4$. The plane-wave calculations were performed with an energy cutoff of 800 eV, and a $2 \times 2 \times 2$ Monkhorst-Pack k-point grid was employed for sampling and numerical integration within the Brillouin zone.⁹

Table S1. Crystal information and structural refinement for KLBO.

Empirical formula	$\text{K}_{7.5}\text{Lu}_{2.5}\text{B}_{15}\text{O}_{30}$
formula weight	4119.15
temperature (K)	293(2)
wavelength (\AA)	0.71073
crystal system	Trigonal
space group	$R\bar{3}2$ (No.155)
a (\AA)	13.1559(6)
b (\AA)	13.1559(6)
c (\AA)	15.0194(11)
Volume (\AA^3)	2251.3(3)
Z	1
density (g/cm^3)	3.038
F (ooo)	1905
R (int)	0.0486
completeness (%)	99.6
GOF on (F^2)	1.014
Final R indices [$F_o^2 > 2\sigma(F_o^2)$] ^a	$R_1=0.0165$, $wR_2 = 0.0328$
R indices (all data)	$R_1= 0.0239$, $wR_2 =0.0338$
CCDC number	2386355
^a $R_1=\sum F_o - F_c /\sum F_o $; $wR_2=[\sum w(F_o^2-F_c^2)^2/\sum w(F_o^2)^2]^{1/2}$	

Table S2. The final atomic coordinates ($\times 10^4$) and equivalent isotropic displacement parameters ($\text{\AA}^2 \times 10^3$) for KLBO, U_{eq} is defined as one-third of the trace of the orthogonalized U_{ij} tensor, and the bond valence sum (BVS) for each atom in asymmetric unit.

Atom	x	y	z	U_{eq}	BVS
Lu(1)	3333	6667	6667	10(1)	2.75
Lu(2)	0	0	7783(1)	8(1)	2.99
K(1)	3333	6667	6667	10(1)	1.79
K(2)	4869(3)	4869(3)	5000	32(1)	0.93
K(3)	2057(2)	3333	3333	26(1)	0.97
K(4)	0	0	5000	24(1)	1.23
O(1)	2801(5)	5222(4)	5499(3)	38(2)	1.74
O(2)	1041(4)	3674(4)	4951(3)	28(1)	2.15
O(3)	1898(5)	3399(4)	6258(3)	33(2)	1.93
O(4)	20(4)	1863(4)	5794(3)	20(1)	2.16
O(5)	1002(4)	1613(3)	7030(2)	16(1)	2.03
B(1)	942(6)	2254(6)	6374(4)	14(2)	3.03
B(2)	1944(10)	4139(6)	5563(4)	21(2)	3.06
B(3)	0	2504(7)	5000	20(2)	3.21

Table S3. Bond lengths (\AA) and angles (deg.) for KLBO.

Lu(1)-O(1)	2.418(5)	K(2)-O(1)#15	3.073(6)
Lu(1)-O(1)#1	2.418(5)	K(2)-O(3)#13	3.119(5)
Lu(1)-O(1)#2	2.418(5)	K(2)-O(3)#1	3.119(5)
Lu(1)-O(1)#3	2.418(5)	K(3)-O(4)#16	2.770(5)
Lu(1)-O(1)#4	2.418(5)	K(3)-O(4)#17	2.770(5)

Lu(1)-O(1)#5	2.418(5)	K(3)-O(5)#13	2.873(4)
Lu(2)-O(5)	2.174(4)	K(3)-O(5)#15	2.873(4)
Lu(2)-O(5)#8	2.174(4)	K(3)-O(2)#18	2.914(5)
Lu(2)-O(5)#9	2.174(4)	K(3)-O(2)	2.914(5)
Lu(2)-O(1)#10	2.292(4)	K(3)-O(3)#15	3.224(6)
Lu(2)-O(1)#11	2.292(4)	K(3)-O(3)#13	3.224(6)
Lu(2)-O(1)#12	2.292(4)	K(4)-O(4)	2.714(4)
K(2)-O(5)#13	2.771(4)	K(4)-O(4)#19	2.714(4)
K(2)-O(5)#1	2.771(4)	K(4)-O(4)#9	2.714(4)
K(2)-O(2)#14	2.859(6)	K(4)-O(4)#8	2.714(4)
K(2)-O(2)#3	2.859(6)	K(4)-O(4)#17	2.714(4)
K(2)-O(1)	3.073(6)	K(4)-O(4)#15	2.714(4)
B(1)-O(3)	1.410(8)	O(5)-Lu(2)-O(1)#11	84.69(18)
B(1)-O(4)	1.368(8)	O(5)#8-Lu(2)-O(1)#11	162.18(17)
B(1)-O(5)	1.323(7)	O(5)#9-Lu(2)-O(1)#11	102.38(18)
B(2)-O(1)	1.306(9)	O(1)#10-Lu(2)-O(1)#11	77.9(2)
B(2)-O(2)	1.379(10)	O(5)-Lu(2)-O(1)#12	102.37(18)
B(2)-O(3)	1.408(8)	O(5)#8-Lu(2)-O(1)#12	84.69(18)
B(3)-O(2)	1.464(7)	O(5)#9-Lu(2)-O(1)#12	162.18(17)
B(3)-O(4)	1.469(7)	O(1)#10-Lu(2)-O(1)#12	77.9(2)
O(1)-Lu(1)-O(1)#1	100.2(2)	O(1)#11-Lu(2)-O(1)#12	77.9(2)
O(1)-Lu(1)-O(1)#2	73.20(16)	O(5)#13-K(2)-O(5)#1	176.5(2)
O(1)#1-Lu(1)-O(1)#2	168.1(3)	O(5)#13-K(2)-O(2)#14	109.83(17)
O(1)-Lu(1)-O(1)#3	73.20(16)	O(5)#1-K(2)-O(2)#14	73.54(14)
O(1)#1-Lu(1)-O(1)#3	114.9(2)	O(5)#13-K(2)-O(2)#3	73.54(14)
O(1)#2-Lu(1)-O(1)#3	73.20(16)	O(5)#1-K(2)-O(2)#3	109.83(17)
O(1)-Lu(1)-O(1)#4	168.1(3)	O(2)#14-K(2)-O(2)#3	49.1(2)
O(1)#1-Lu(1)-O(1)#4	73.20(16)	O(5)#13-K(2)-O(1)	61.74(12)
O(1)#2-Lu(1)-O(1)#4	114.9(2)	O(5)#1-K(2)-O(1)	116.80(13)

O(1)#3-Lu(1)-O(1)#4	100.2(2)	O(2)#14-K(2)-O(1)	134.42(15)
O(1)-Lu(1)-O(1)#5	114.9(2)	O(2)#3-K(2)-O(1)	88.17(13)
O(1)#1-Lu(1)-O(1)#5	73.20(16)	O(5)#13-K(2)-O(1)#15	116.80(13)
O(1)#2-Lu(1)-O(1)#5	100.2(2)	O(5)#1-K(2)-O(1)#15	61.74(12)
O(1)#3-Lu(1)-O(1)#5	168.1(3)	O(2)#14-K(2)-O(1)#15	88.17(13)
O(1)#4-Lu(1)-O(1)#5	73.20(16)	O(2)#3-K(2)-O(1)#15	134.42(15)
O(5)-Lu(2)-O(5)#8	95.37(14)	O(1)-K(2)-O(1)#15	136.9(2)
O(5)-Lu(2)-O(5)#9	95.37(14)	O(5)#13-K(2)-O(3)#13	46.38(11)
O(5)#8-Lu(2)-O(5)#9	95.37(14)	O(5)#1-K(2)-O(3)#13	133.48(11)
O(5)-Lu(2)-O(1)#10	162.18(17)	O(2)#14-K(2)-O(3)#13	92.38(15)
O(5)#8-Lu(2)-O(1)#10	102.38(18)	O(2)#3-K(2)-O(3)#13	90.59(15)
O(5)#9-Lu(2)-O(1)#10	84.69(18)	O(1)-K(2)-O(3)#13	104.77(13)
O(1)#15-K(2)-O(3)#13	73.98(12)	O(4)#16-K(3)-O(3)#13	97.51(12)
O(5)#13-K(2)-O(3)#1	133.48(11)	O(4)#17-K(3)-O(3)#13	158.89(13)
O(5)#1-K(2)-O(3)#1	46.38(11)	O(5)#13-K(3)-O(3)#13	44.71(12)
O(2)#14-K(2)-O(3)#1	90.59(15)	O(5)#15-K(3)-O(3)#13	98.92(13)
O(2)#3-K(2)-O(3)#1	92.38(15)	O(2)#18-K(3)-O(3)#13	111.04(13)
O(1)-K(2)-O(3)#1	73.98(12)	O(2)-K(3)-O(3)#13	122.79(13)
O(1)#15-K(2)-O(3)#1	104.77(13)	O(3)#15-K(3)-O(3)#13	65.62(17)
O(3)#13-K(2)-O(3)#1	176.7(2)	O(4)-K(4)-O(4)#19	127.56(18)
O(4)#16-K(3)-O(4)#17	101.50(19)	O(4)-K(4)-O(4)#9	102.13(11)
O(4)#16-K(3)-O(5)#13	74.46(12)	O(4)#19-K(4)-O(4)#9	125.70(18)
O(4)#17-K(3)-O(5)#13	133.33(12)	O(4)-K(4)-O(4)#8	102.13(11)
O(4)#16-K(3)-O(5)#15	133.33(12)	O(4)#19-K(4)-O(4)#8	52.17(18)
O(4)#17-K(3)-O(5)#15	74.46(12)	O(4)#9-K(4)-O(4)#8	102.13(11)
O(5)#13-K(3)-O(5)#15	141.40(18)	O(4)-K(4)-O(4)#17	52.17(18)
O(4)#16-K(3)-O(2)#18	49.33(13)	O(4)#19-K(4)-O(4)#17	102.13(11)
O(4)#17-K(3)-O(2)#18	88.49(14)	O(4)#9-K(4)-O(4)#17	127.56(18)
O(5)#13-K(3)-O(2)#18	117.29(12)	O(4)#8-K(4)-O(4)#17	125.70(18)

O(5)#15-K(3)-O(2)#18	84.02(12)	O(4)-K(4)-O(4)#15	125.70(19)
O(4)#16-K(3)-O(2)	88.50(14)	O(4)#19-K(4)-O(4)#15	102.13(11)
O(4)#17-K(3)-O(2)	49.33(13)	O(4)#9-K(4)-O(4)#15	52.17(18)
O(5)#13-K(3)-O(2)	84.02(12)	O(4)#8-K(4)-O(4)#15	127.56(18)
O(5)#15-K(3)-O(2)	117.29(12)	O(4)#17-K(4)-O(4)#15	102.13(11)
O(2)#18-K(3)-O(2)	115.2(2)	O(5)-B(1)-O(4)	123.9(6)
O(4)#16-K(3)-O(3)#15	158.89(13)	O(5)-B(1)-O(3)	117.9(6)
O(4)#17-K(3)-O(3)#15	97.51(12)	O(4)-B(1)-O(3)	118.2(5)
O(5)#13-K(3)-O(3)#15	98.92(13)	O(1)-B(2)-O(2)	121.2(7)
O(5)#15-K(3)-O(3)#15	44.71(12)	O(1)-B(2)-O(3)	121.6(8)
O(2)#18-K(3)-O(3)#15	122.79(13)	O(2)-B(2)-O(3)	117.3(6)
O(2)-K(3)-O(3)#15	111.05(13)	O(2)-B(3)-O(2)#17	108.5(7)
O(2)-B(3)-O(4)#17	108.2(3)	O(2)#17-B(3)-O(4)	108.2(3)
O(2)#17-B(3)-O(4)#17	111.6(2)	O(4)#17-B(3)-O(4)	108.7(7)
O(2)-B(3)-O(4)	111.6(2)	O(5)-B(1)-O(4)	123.9(6)

Symmetry transformations used to generate equivalent atoms:

#1 $-x+2/3, -x+y+1/3, -z+4/3$ #2 $-x+y, -x+1, z$ #3 $-y+1, x-y+1, z$
#4 $x-y+2/3, -y+4/3, -z+4/3$ #5 $y-1/3, x+1/3, -z+4/3$
#6 $y+1/3, x+2/3, -z+5/3$ #7 $x+1/3, y+2/3, z-1/3$ #8 $-y, x-y, z$
#9 $-x+y, -x, z$ #10 $x-1/3, y-2/3, z+1/3$ #11 $-y+2/3, x-y+1/3, z+1/3$
#12 $-x+y-1/3, -x+1/3, z+1/3$ #13 $-x+y+1/3, -x+2/3, z-1/3$
#14 $x-y+1, -y+1, -z+1$ #15 $y, x, -z+1$ #16 $-y+1/3, x-y+2/3, z-1/3$
#17 $-x, -x+y, -z+1$ #18 $x-y+1/3, -y+2/3, -z+2/3$ #19 $x-y, -y, -z+1$

Table S4 Direction and magnitude of the dipole moments in $K_{7.5}Lu_2B_{15}O_{30}$.

Compound	Species	Dipole moments (Debye)			Dipole moments (Debye)
		x	y	z	
$K_{7.5}Lu_{2.5}B_{15}O_{30}$	Lu ₍₁₎ O ₆	0.0001	-0.0015	-3.9248	3.9248
		0.0001	-0.0026	-2.5963	2.5963
	Lu ₍₂₎ O ₆	-0.0008	-0.0003	0.0008	0.0011
		0.0000	0.0000	0.0000	0.0000
	B ₍₁₎ O ₃	-0.8827	0.7159	-0.6337	1.3013

		-0.9967	-1.1379	3.5073	3.8196
	$B_{(2)}O_3$	0.5257	0.1915	-2.0814	2.1553
		0.5378	2.2801	-0.0886	2.3443
	$B_{(3)}O_4$	-0.0786	0.1596	-0.0005	0.1778

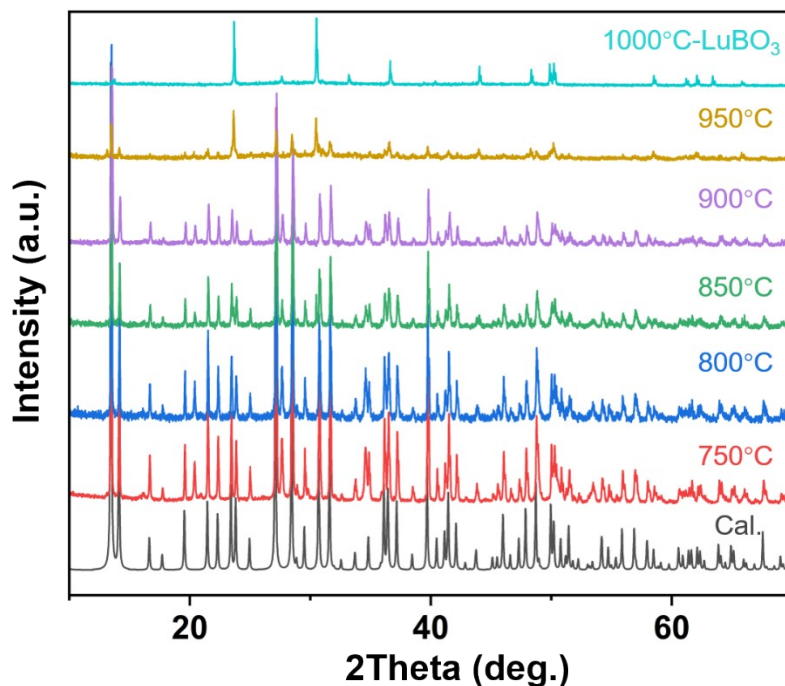


Fig. S1 Variable-temperature PXRD measurements of KLBO.

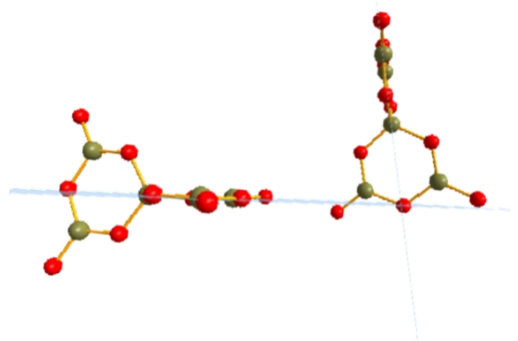


Fig. S2 Dihedral angle of the $[B_5O_{10}]$ groups in KLBO.

References.

- (1) G. M. Sheldrick, SHELXT-Integrated space-group and crystal structure determination. *Acta Crystallogr. Sect. A Found. Crystallogr.*, 2015, **71**, 3-8.
- (2) A. L. Spek, Single-crystal structure validation with the program PLATON. *J. Appl. Crystallogr.*, 2003, **36**, 7-13.
- (3) Spek. A. L, Single-Crystal Structure Validation with the Program PLATON. *J. Appl. Crystallogr.* 2003, **36**, 7-13.
- (4) T. H. Zhang, L. L. Li, J. Chai, H. T. Zhou, N. Ye, Z. G. Hu, Y. C. Wu, C.G. Li, A defect

pyrochlore-like acentric cubic lead titanium-tellurate crystal exhibiting strong second harmonic generation activity and an extended transparent window. *Inorg. Chem. Front.*, 2024, **11**, 7374-7381.

- (5) S. K. Kurtz and T. T. Perry, A powder technique for the evaluation of nonlinear optical materials. *J. Appl. Phys.*, 1968, **39**, 3798-3813.
- (6) S. J. Clark, M. D. Segall, C. J. Pickard, P. J. Hasnip, M. J. Probert, K. Refson and M. C. Payne, First Principles Methods Using CASTEP. *Z. Kristallogr-Cryst. Mater.*, 2005, **220**, 567.
- (7) V. Milman, K. Refson, S. J. Clark, C. J. Pickard, J. R. Yates, S. P. Gao, P. J. Hasnip, M. I. J. Probert, A. Perlov and Segall, M. D, Electron and vibrational spectroscopies using DFT, plane waves and pseudopotentials: CASTEP implementation. *J. Mol. Struct., THEOCHEM*. 2010, **954**, 22-35.
- (8) W. Kohn, Electronic structure of matter-wave functions and density functionals. *Rev. Mod. Phys.*, 1999, **71**, 1253-1266.
- (9) H. J. Monkhorst and J. D. Pack, Special points for Brillouin-zone integrations. *Matter Mater. Phys.*, 1976, **13**, 5188-5192.